Bull. Chem. Soc. Ethiop. **2020**, 34(2), 323-334. ISSN 1011-3924
© 2020 Chemical Society of Ethiopia and The Authors Printed in Ethiopia
DOI: https://dx.doi.org/10.4314/bcse.v34i2.10

SYNTHESIS OF CuO-NPS BY SIMPLE WET CHEMICAL METHOD USING VARIOUS DICARBOXYLIC ACID SALTS AS PRECURSORS: SPECTRAL CHARACTERIZATION AND *IN-VITRO* BIOLOGICAL EVALUATION

Hajira Rehman[1], Zulfiqar Ali[2], Abdul Qadir[3], M. Hassan Farooq[2*], Ahmed Shuaib[2], Asmat Zahra[4], Tanzeela Shahzady[3] and Habib Hussain[5]

[1]Department of Chemistry, University of Sahiwal, Sahiwal, Pakistan
[2]Department of Basic Sciences & Humanities University of Engineering & technology Lahore KSK Campus, Pakistan
[3]Department of Chemistry Lahore Garrison University, Lahore, Pakistan
[4]Institute of Chemistry, University of The Punjab, Lahore, Pakistan
[5]Department of Basic Sciences & Humanities University of Engineering & Technology Lahore Narowal Campus, Pakistan

(Received September 9, 2019; Revised September 28, 2020; Accepted October 1, 2020)

ABSTRACT. In this study, a simple chemical reduction method was employed to synthesize CuO-NPs. Various dicarboxylic acids were converted into Cu(II) salt of dicarboxylic acid which were used as precursors. NPs were produced by reducing precursors with $NaBH_4$. Characteristics of synthesized NPs were investigated by using important analytical techniques including Fourier transform infrared (FTIR) spectroscopy, X-ray diffraction (XRD), thermo gravimetric analysis (TGA) and scanning electron microscopy (SEM). Developed NPs were investigated for their antibacterial activity against a range of bacterial strains by employing agar well diffusion method. CuO-NPs exhibited good to moderate activity against *E-Coli*, *B. Subtilis* and poor activity against *K. pneumonia* and Methicillin-resistant *Staphylococcus aureus* (MRSA). It was found that amongst all experienced compounds sample 2 showed good activity with minimum inhibition concentration (MIC) 10 µg/mL (zone of inhibition: 22± 0.12 mm) while sample 3 showed poor activity with MIC 40 µg/mL (zone of inhibition: 8.0 ± 0.18 mm).

KEY WORDS: CuO-NPs, Dicarboxylic acids, Sodium borohydride, Antibacterial study

INTRODUCTION

Now a day's modern research is revolving around nanotechnology because nanoparticles have unique catalytic [1] and bio-medical applications [2, 3]. CuO-NPs are of great interest than other metal NPs due to its low cost and easy availability. Copper oxide nanomaterials have been developed substantially in recent years due to its low cost fabrication and good electrochemical properties. Copper oxides NPs are used for gas sensors [4], photovoltaic solar cell [5, 6], photo electrochemical cell [7, 8] and electro-chromic coatings [9].

Metal oxide NPs mainly dragged the attention of researchers due to their medicinal applications. Metal oxides exhibited excellent antimicrobial and antifungal activities against various organisms [10-12]. Metallic NPs have immense surface area and this surface area and particle size play a key role in medicinal, catalytic activities and photocatalytic degradation [13], that is why comparison of metallic NPs surface area with conventional materials have been intensely investigated [14].

Now a day there is a common use of antibacterial agents in various fields including, food packaging, textile industry, water disinfection and medicine [15]. Over dosing of antibiotics has resulted in increased bacterial strains having antibiotic resistant genes. In order to resolve this problem, a great deal of research has been done. NPs exhibit a range of potentially useful

*Corresponding author. E-mail: mhfarooq@uet.edu.pk

applications for pharmaceutical purposes. In last few decades, nanotechnology has great interest in evaluating activity of nano-scale metals as antimicrobial agents.

Antimicrobial study of different metallic NPs such as alumina [16], silver [17], iron [18, 19], gold [20, 21], magnesium [22, 23], titanium [24], and zinc oxide [25] were investigated on large scale. Although tremendous efforts have been done to utilize NPs as an antibacterial agent, still we are not able to develop ideal metallic NPs with proficient activity. In this research an effort is made to find out a quick and easy method to synthesize CuO-NPs. Dicarboxylic acid salts are used as precursors to synthesize the target materials and their antimicrobial activities were investigated against different pathogenic strains of bacteria.

EXPERIMENTAL

Synthesis of CuO-NPs by using copper(II) succinate precursor

By following procedure adopted by Arunachalam *et al.* [26], 2.5 g of $CuSO_4.5H_2O$ was taken and dissolved in distilled water (20 mL) in a beaker equipped with magnetic stirrer to form a homogeneous mixture. In order to prepare sodium succinate, 0.80 g of sodium hydroxide and 1.18 g succinic acid were mixed in a beaker having 10 mL distilled water. Prepared sodium succinate was introduced in copper sulfate solution drop wise under continues magnetic stirring. Resulting solution was magnetically stirred for 50 min and a green precipitate of copper(II) succinate was collected which was further centrifuged, washed several times with ethanol and then product was dried.

In order to make final product, solution of $NaBH_4$ was prepared by adding 1.3 g of it in 10 mL distilled water. 1.80 g copper succinate dissolved in 10 mL distilled water and $NaBH_4$ solution was added drop wise to this solution with stirring. Reaction mixture was kept in the ultrasonic bath for 60 min. Formation of copper oxide nanoparticles was confirmed by turning green colored solution instantly into black upon addition of $NaBH_4$ solution [26]. Copper oxide nanoparticles thus formed, filtered and dried.

Synthesis of CuO-NPs by using copper(II) adipiate precursor

Solution of $CuSO_4.5H_2O$ was prepared by dissolving 2.5 g of it in distilled water in a beaker equipped with magnetic stirrer. In another beaker, 0.80 g of sodium hydroxide accurately weighed and 1.46 g of adipic acid in 10 mL distilled water were mixed to form sodium adipiate solution. Sodium adipiate thus formed was added drop wise to copper sulphate solution under stirring which was continued for 50 min and at end a dark green precipitate of copper(II) adipiate was obtained. These precipitates were washed followed by centrifugation and then dried. In the 2^{nd} step, 1.3 g of $NaBH_4$ dissolved in 10 mL distilled water and introduced drop wise into copper(II) adipiate solution prepared by adding 2.07 g of this salt into distilled water of volume 10 mL and solution was kept in ultrasonic bath for 1 hour. When $NaBH_4$ solution was added dark green colored solution instantly turned dark brown which indicated the formation of CuO-NPs. Nanoparticles thus formed, filtered and dried.

Synthesis of CuO-NPs by using copper(II) malonate precursor

Copper sulfate solution was prepared by taking 2.5 g of it in 20 mL distilled water in a beaker equipped with magnetic stirrer to form a homogeneous mixture. In order to prepare sodium malonate, 0.80 g of sodium hydroxide and 1.04 g malonic acid was dissolved in 10 mL distilled water in a beaker. Sodium malonate thus formed was added in copper sulfate solution under constant stirring. Magnetic stirring of solution continued for 40-50 min and a green precipitate of copper(II) malonate was collected, washed, centrifuged and dried.

$NaBH_4$ solution and solution of copper(II) malonate were prepared separately by dissolving 1.3 g and 1.65 g of both materials, respectively, in 10 mL distilled water. Then two solutions were mixed into each other drop wise and resulting solution was kept in ultrasonic bath for 60 min. Upon addition of sodium borohydride, green colored solution turned black, which indicated the formation of CuO-NPs. Nanoparticles thus formed, filtered and dried.

Experimental procedure of antimicrobial activity

Antimicrobial study of synthesized NPs was based on following steps:

Preparation of the test compound

2 mg of NPs (each sample separately) were dissolved in 1 mL of ethanol which was further diluted of varying concentrations, i.e. (0.2 mg/0.1 mL, 0.02 mg/0.1 mL, and 0.002 mg/0.1 mL) for microbiological assays.

LB broth preparation

LB broth is prepared (without agar), shifted in five test tubes, each containing 5 mL broth and autoclaved. Inoculation of five bacterial strains were done in these test tubes and placed on shaker for 24 hours.

Preparation of agar plates and microbiological assays

Severe sterilized and aseptic conditions were maintained and procedure was done in laminar airflow. Applying the agar plate diffusion technique test organisms was grown in LB nutrient agar medium. The composition of the medium was (g/L) tryptone (1.0 g), yeast extract (0.5 g), sodium chloride (0.5 g); agar (1.5- 2 g) and water (100 mL). CuO-NPs synthesized by three different precursors were tested according to pre mentioned concentration by dissolving in ethanol, while ethanol itself was used as control for comparison.

N-agar media was autoclaved and 25-30 mL of the media was added into the 9 cm diameter Petri-dish, allowed to solidify and then one ml bacterial suspension was transferred/plate incubated at 27 ^{o}C for 24 hours. The wells were made in the plates with the help of autoclaved pasture pipette and then it was filled with the synthesized CuO-NPs solution. The 100 µg/mL concentration of NPs was used and activity was determined by measuring the inhibition zone.

RESULTS AND DISCUSSION

IR studies of CuO NPs

IR spectrum of synthesized CuO NPs by using malonic acid, succinic acid and adipic acid precursor were recorded. Since water is adsorbed on metal surface in nanoparticles that is why two characteristic absorption peaks were expected, one of them above 3000 cm^{-1} which was not prominent in malonic acid precursor spectrum and second peak at 1119.00 cm^{-1}. In this spectrum 1st peak was not prominent but 2nd peak was quit prominent. This 2nd prominent peak might be due to –OH twisting frequency. In succinic acid precursor spectrum two characteristic absorption peaks were recorded at 3261.20 and 1113.00 cm^{-1} which might be due to –OH stretching and twisting frequencies respectively due to adsorbed water molecules. Similarly adipic acid precursor spectrum also exhibited these two characteristic absorption peaks at 3403.00 and 1120.40 cm^{-1}. Literature proved that M–O stretching and twisting vibrations were seen beneath 1000 cm^{-1} so IR spectra bellows this range of our interest. Crest in malonic acid

precursor spectrum at 620.32 cm^{-1} is considered due to Cu–O str-frequency [27] which is a decent proof of development of Cu–O linkage in synthesized nanoparticles. Similarly in other two spectra, peaks recognized at 612.33 cm^{-1} and 598.16 cm^{-1}, respectively, are associated with Cu–O stretching [28].

XRD studies of CuO NPs:

Powder XRD analysis of sample 1

XRD analysis of synthesized NPs was carried on X-ray powder diffractometer under 45 kV/40 mA X-ray, $2\theta^{/0}$ scanning mode, fixed monocharomator with a range from $2\theta^{/0}$ = 10 to 90 with a step of 0.02 degree for a period of 30 min as shown in Figure 1. Eight peaks were selected and miller indices were calculated for them as shown in Table 1.

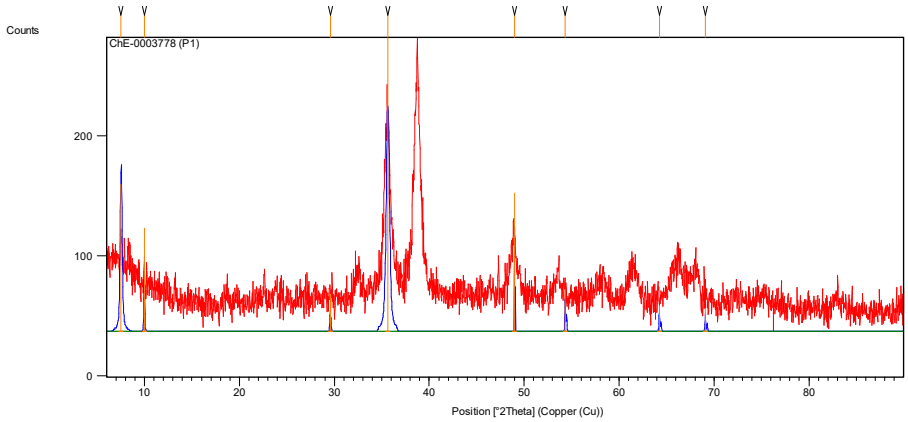

Figure 1. XRD spectra of NPs (Sample 1).

Table 1. Calculation of miller indices through XRD diffraction pattern.

$2\theta^{/0}$	$\theta^{/0}$	$Sin^2\theta$	1x $\frac{Sin^2\theta}{Sin^2\theta_{min}}$	2x $\frac{Sin^2\theta}{Sin^2\theta_{min}}$	3x $\frac{Sin^2\theta}{Sin^2\theta_{min}}$	Whole integers	*Hkl*
7.5487	3.7742	0.00433	1	2	3	3	111
9.9686	4.9843	0.00758	1.7509	3.5013	5.1939	5	210
29.5423	14.7711	0.06500	15.0115	30.0230	45.0345	45	542
36.9967	18.4983	0.10066	23.2363	46.4456	69.7091	70	653
49.5321	24.7660	0.17547	40.4893	80.9786	121.468	121	766
55.3230	27.6615	0.21552	49.7736	99.5472	149.3208	149	876
64.0010	32.0005	0.28082	64.8545	130.1477	194.5635	194	987
69.6703	34.8351	0.32628	75.3533	150.7066	226.0599	226	998

Miller indices of synthesized nanoparticles were calculated for by using malonic acid precursor from selected peaks as shown in Table 1. Calculated and reported pattern of CuO nanoparticles was compared by peak search method and presented great resemblance. All major peaks at positions $2\theta^{/o}$ 7.5487, 9.9686, 29.5423, 36.9967, 49.5321, 55.3230, 64.0010, 69.6703 have miller indices 111, 210, 542, 653,766,876, 987, 998, respectively, which are the characteristics of CuO scan pattern.

Material parameters were calculated with the help of $2\theta/^0$ values and grain size was found to be in range of 9.0561 nm to at $2\theta/^0$ = 7.5487 to 33.9828 nm at $2\theta/^0$ = 69.6703.

Powder XRD analysis of sample 2

X-ray powder diffraction analysis of sample 2 was carried out by following same conditions and parameters which were employed for sample 1. For this sample total seven peaks were targeted and calculated their miller indices as shown in Table 2.

Table 2. Calculation of miller indices through XRD diffraction Pattern.

$2\theta/^0$	$\theta/^0$	$Sin^2\theta$	1x $\frac{Sin^2\theta}{Sin^2\theta_{min}}$	2x $\frac{Sin^2\theta}{Sin^2\theta_{min}}$	3x $\frac{Sin^2\theta}{Sin^2\theta_{min}}$	Whole integers	*Hkl*
6.5506	3.2753	0.00326	1	2	3	3	111
10.8075	5.4037	0.00886	2.7177	5.4354	8.1531	8	220
13.6687	6.8343	0.01416	4.3435	8.6870	13.0305	13	320
24.4260	12.2130	0.04475	13.7269	27.4538	41.1809	41	540
25.6642	12.7321	0.04857	14.8987	29.7974	44.6961	45	630
33.0136	16.5068	0.08072	24.7607	49.5214	74.2821	74	750
44.0968	22.0484	0.14091	43.2239	86.4478	129.6717	130	970

The miller indices of synthesized nanoparticles by using succinic acid precursor have been calculated from selected peaks as shown in Table 2. The calculated pattern of CuO nanoparticles was compared with reported patterns (present in the library) by peak search method and showed great resemblance. All the major peaks at positions $2\theta/^o$ 6.5506, 10.8075, 13.6687, 24.4260, 25.6642, 33.0136, 44.0968 have miller indices 111, 220, 320, 540, 630, 750, 970, respectively, which are the characteristics of CuO scan pattern.

After performing calculations, grain size was found to be in the range of 9.0502 nm at $2\theta/^0$ = 6.5506 to 13.9067 nm at $2\theta/^0$ = 25.6642.

Powder XRD analysis of sample 3

Sample 3 was also by following same conditions and parameters of X-ray diffractometer which were employed for sample 1. For this sample 8 prominent peaks were taken for calculating their miller indices, data presented in Table 3.

Table 3. Calculation of miller indices through XRD diffraction pattern.

$2\theta/^0$	$\theta/^0$	$Sin^2\theta$	1x $\frac{Sin^2\theta}{Sin^2\theta_{min}}$	2x $\frac{Sin^2\theta}{Sin^2\theta_{min}}$	3x $\frac{Sin^2\theta}{Sin^2\theta_{min}}$	Whole integers	*Hkl*
7.6370	3.8185	0.00443	1	2	3	3	111
12.8423	6.4211	0.01250	2.8216	5.6432	8.4648	8	220
14.5882	7.2941	0.01611	3.6590	7.8181	10.9772	11	311
19.0634	9.5317	0.02742	6.2272	12.4545	18.6818	19	331
21.4065	10.7032	0.03449	7.8386	15.6772	23.5159	24	422
31.6605	15.8302	0.07441	16.7968	33.5936	50.3904	50	543
47.6014	23.8007	0.16285	36.7607	73.5214	110.2821	110	765
62.1894	31.0947	0.26672	60.2076	120.4152	180.6228	181	986

Miller indices of synthesized nanoparticles by using Adipic acid precursor have been calculated from selected peaks. Calculated pattern of CuO nanoparticles was matched with reported patterns (present in the library) by peak search method and showed great resemblance. All main peaks at positions $2\theta/^o$ 7.6370, 12.8423, 14.5882, 19.0634, 21.4065, 31.6605, 47.6014,

62.1894 have miller indices 111, 220, 311, 331, 422, 543, 765, 986, respectively, which are the characteristics of CuO scan pattern.

In this sample grain size was found to be 11.2723 nm at $2\theta^{/0}$ = 31.6605 to 13.7549 nm at $2\theta^{/0}$ = 19.0634. X- ray diffraction analysis showed that CuO NPs were synthesized with varying sizes by using three different precursors. The smallest particle sizes with highest surface area were recorded for those NPs (sample 2) which were synthesized by using succinic acid as a precursor.

SEM analysis

Sample 1. SEM image shown in Figure 2 was utilized in order to reveal surface morphology of CuO nanoparticles synthesized in this project recorded at 25 kx (Figure 2a) and 10 kx (Figure 2b) magnifications respectively. Both figures belong to same sample but with different magnifications.

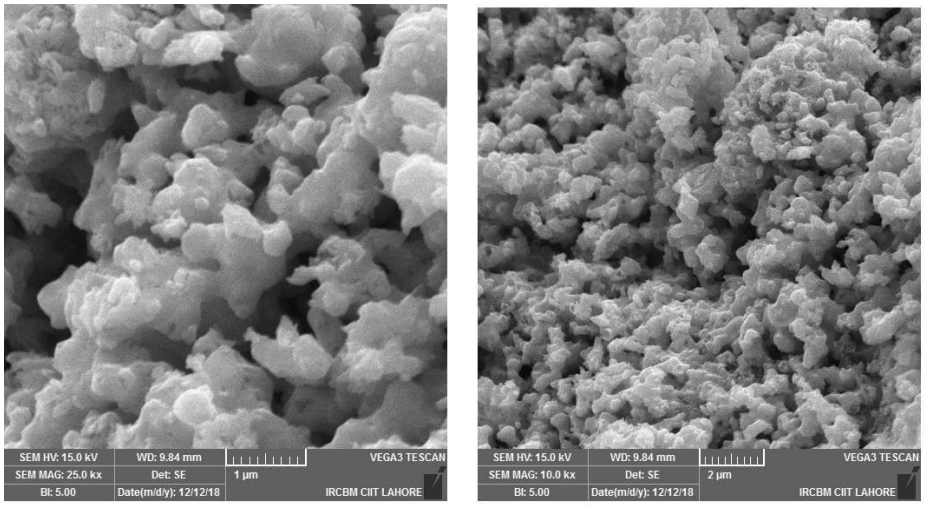

Fig (a) Fig (b)

Figure 2. SEM image CuO NPs from malonic acid as precursor.

It is obvious from above diagram that large number of CuO nanosphere agglomerates with a uniform size. Similarly non-agglomerated random shape particles aggregate to give a flower shape structure of synthesized NPs.

Sample 2. Surface morphology of CuO nanoparticles recorded at various magnifications through SEM analysis are shown in Figure 3.

It is obvious from above SEM images that particles are spherical and dispersed in a good manner having a properly and well defined homogeneous crystalline structure. SEM is also showing good tendency of these particles for agglomerations. A regular polyhedron shape for the CuO-NPs can be seen in above SEM images. Island growth of firmly packed spherical arrangement is also observed clearly. However there are some regions were big nanoparticles are surrounded by smaller nanoparticles. Similar CuO-NPs SEM images were taken into record and reported [29].

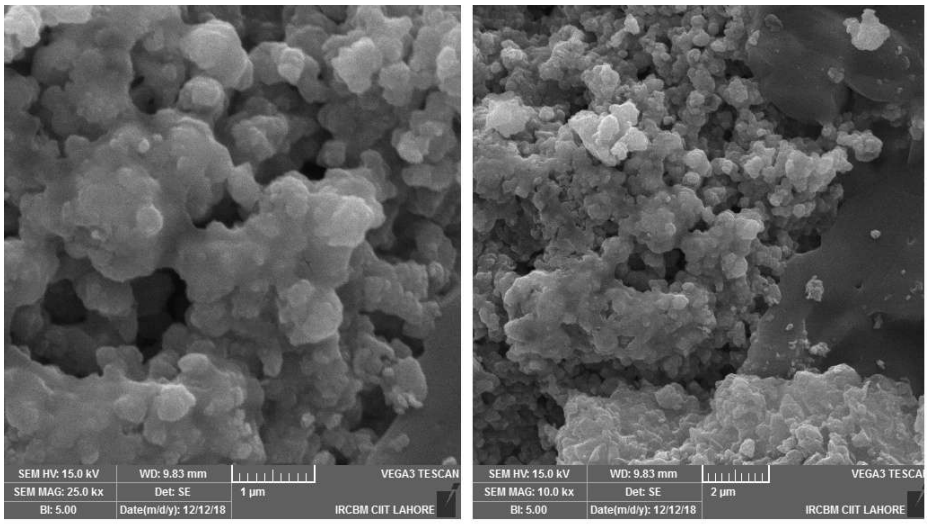

Fig (a) Fig (b)

Figure 3. SEM image CuO NPs from succinic acid as a precursor.

Sample 3. Surface morphology of CuO nanopartices recorded at various magnifications through SEM analysis is shown in Figure 4.

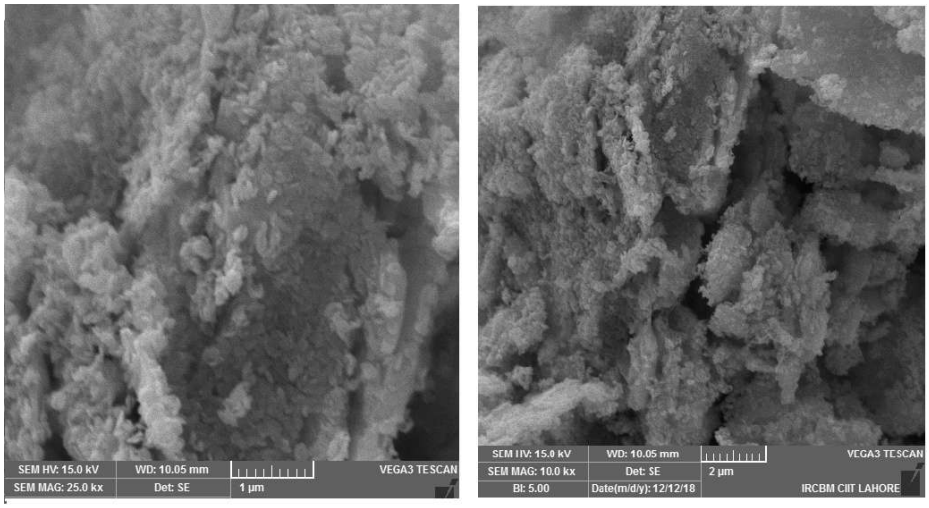

Fig (a) Fig (b)

Figure 4. SEM image CuO NPs from adipic acid as precursor.

It is clear from above diagram that particles are well defined, shows spherical and identical crystalline structure. It seems that synthesized particles are agglomerated and form a cluster. Particle size in SEM images of all three samples was found in the range of 1-2 µm.

TGA analysis

The decomposition pattern was recorded from TGA/DSC analysis of synthesized materials. NPs synthesized from malonic acid precursor, succinic acid precursor and adipic acid precursor are labeled as a, b and c, respectively.

TGA and DSC studies of CuO NPs were done in nitrogen atmosphere. The synthesized NPs by using different precursors showed very similar decomposition pattern. For material labeled **a**, 1st weight loss was recorded between 50 °C and 160 °C which may be due to removal of physically absorbed and chemically bonded water with synthesized NPs. The two endothermic DSC peaks around 75 °C and 170 °C confirmed the evaporation of water. This weight loss pattern showed good agreement with the TGA results [30, 31]. Materials labeled as **b** and **c** showed approximate same pattern in the above mentioned temperature range. In material **a**, there is another weight loss around 280 °C which may be ascribed to the loss of the decomposition of few residual impurities along with DSC peak around 310 °C. Materials **b** and **c** also showed same response in this temperature range. After 300 °C to onward, there is no significant weight loss by increasing temperature in all three samples. This behavior indicated the thermal stabilization of the synthesized CuO NPs.

Antimicrobial activity of CuO-NPs

In latest study in nanotechnology, various metal and metal oxide nanoparticles have been reported as antimicrobial agent [32-40]. Metal nanoparticles containing magnesium oxide [34], copper [38, 40], silver [32-36], iron [41], zinc oxide [42-44], and nickel oxide [45, 46] are exhibit antimicrobial properties. Antimicrobial activity of CuO nanoparticles synthesized by using different precursors were tested against three gram positive bacterial strains, i.e. *S. aureus*, *B. subtilis*, *MRSA* and three gram-negative strains, i.e. *E. coli*, *S. typhi*, and *K. pneumoniae* by using the agar well diffusion assay method [47]. Results are presented in Table 4.

Table 4. Zone of inhibition of CuO-NPs against pathogenic bacterial strains.

Sample	Diameter of inhibition zone (mm)					
	Gram Positive			Gram Negative		
	S. aureus	*B. subtilis*	*MRSA*	*E. coli*	*K. pneumoniae*	*S. typhi*
Sample 1	12±0.11	25±2.50	5.0±0.51	20±0.1	8.0±0.13	10±0.55
Sample 2	18±1.1	22±0.12	10±0.33	25±0.02	10±0.11	15±0.12
Sample 3	15±.15	20±0.11	8.0±0.18	22±0.41	10±0.15	12±0.17
Standard[a]	30±0.11	28±0.21	32±0.51	29±0.06	28±0.17	26±0.01

[a]Ampicillin was used as positive control.

CuO-NPs showed good antibacterial activity against selected bacterial strains. NPs found to be more effective against *B. Subtilis* and *S. aureus* and reluctant their growths to a greater extent but these particles were found to be less effective against *MRSA*. Similarly activity of CuO-NPs was found to be quite promising and encouraging against *E. coli* but less diameter of inhibition zone was noticed in case of *K. pneumoniae* and *S. typhi*. MIC values in µg/mL were calculated, comparing it with standard antibacterial (Ampicillin) in concentration 1.0 µg/mL in each plate as positive control. Results are summarized in Table 5.

The MIC value of sample 1 is maximum, i.e. 35 µg for *K. pneumoniae* and minimum, i.e. 15 µg for *B. Subtilis* and *E. coli*. Similarly, sample 2 surprisingly showed very small MIC value against *E. coli* which is an effectiveness indicator of this sample against this strain. Sample 3 showed higher MIC value, i.e. 40 µg against *K. pneumonia*, which indicates the less activity of this sample against concerned bacterial strain.

Table 5. MIC of CuO-NPs against pathogenic bacterial strains.

Sample	MIC values against various bacterial strains (µg/mL)					
	Gram Positive			Gram Negative		
	S. aureus	*B. Subtilis*	*MRSA*	*E. coli*	K. pneumoniae	*S. typhi*
Sample 1	25	15	30	15	35	25
Sample 2	11	10	25	5	30	15
Sample 3	30	35	25	10	40	10
Standard[a]	7	5	8	9	6	8

[a]Ampicillin was used as positive control.

It can be concluded that CuO nanoparticles can inhibit bacterial cell growth and multiplication. This inhibition in growth may be due to the phenomenon in which NPs adhere to cell wall of bacteria and penetrated through cell membrane, which finally leads to cell lysis. This resulted into inhibition of bacterial cell growth and multiplication. As a result, it is highly recommended that use of CuO-NPs as an economic alternative anti- bacterial agent especially in treating ectopic infections.

CONCLUSION

Using a simple and inexpensive wet chemical method, synthesis of copper oxide nanoparticals with size of 1-2 µm has been successfully carried out. FTIR, XRD and SEM results confirmed successful synthesis of CuO-NPs. Powder X-ray analysis showed that NPs synthesized from succinic acid salt precursor have smallest sizes and larger surface area. Remarkable activity against various bacterial strains were exhibited by sample 2 with MIC 10 µg/mL and zone of inhibition 22±0.12 against *B. Subtilis* indicating that these synthesized NPs are good candidates for future therapeutic applications in medical field.

ACKNOWLEDGMENTS

Authors gratefully acknowledge the Chairman BS and Head of Department, UET Lahore (KSK Campus) to provide lab facility to carry out this research work. We are also thankful to Comsat Institute of Information & Technology Lahore, Pakistan for assisting us in sample characterization.

REFRENCES

1. Moreno-Manas, M.; Pleixats, R. Formation of carbon−carbon bonds under catalysis by transition-metal nanoparticles. *Acc. Chem. Res*. **2003**, 36, 638-643.
2. Lanone, S.; Boczkowski, J. Biomedical applications and potential health risks of nanomaterials: Molecular mechanisms. *Curr. Mol. Med*. **2006**, 6, 651-663.
3. Garnett, M.C.; Kallinteri, P. Nanomedicines and nanotoxicology: Some physiological principles. *Occup. Med*. **2006**, 56, 307-311.
4. Hoa, N.D.; An, S.Y.; Dung, N.Q.; Quy, N.V.; Kim, D. Synthesis of p-type semiconducting cupric oxide thin films and their application to hydrogen detection. *Sens. Actuators B* **2010**, 146, 239-244.
5. Wong, L.M.; Chiam, S.Y.; Huang, J.Q.; Wang, S.J.; Pan, J.S.; Chim, W.K. Growth of Cu_2O on Ga-doped ZnO and their interface energy alignment for thin film solar cells. *J. Appl. Phys*. **2010**, 108, 033702. https://doi.org/10.1063/1.3465445
6. Mebrahtu, C.; Taddesse, A.M.; Goro, G.; Yohannes, T. Natural pigment sensitized solar cells based on ZnO-TiO_2-Fe_2O_3 nanocomposite in quasi-solid state electrolyte system. *Bull. Chem. Soc. Ethiop*. **2017**, 31, 263-279.

7. Mahalingam, T.; Chitra, J.S.P.; Chu, J.P.; Moon, H.; Kwon, H.J.; Kim, Y.D. Photoelectrochemical solar cell studies on electroplated cuprous oxide thin films. *J. Mater. Sci.: Mater. Electron.* **2006**, 17, 519-523.
8. Fernando, C.A.N.; Bandara, T.M.W.J.; Wethasingha, S.K. H_2 evolution from a photoelectrochemical cell with n-Cu_2O photoelectrode under visible light irradiation. *Sol. Energy Mater*. *Sol. Cells* **2001**, 70, 121-129.
9. Ristova, M.; Neskovska, R.; Mireski, V. Chemically deposited electrochromic cuprous oxide films for solar light modulation. *Sol. Energy Mater. Sol. Cells* **2007**, 91, 1361-1365.
10. Wei, B.; Shi, Z.; Xiao, J.; Xu, Y.; Lv, L. *In vivo* and *in vitro* antibacterial effect of nano-structured titanium coating incorporated with silver oxide nanoparticles. *J. Biomater. Tiss. Eng*. **2017**, 7, 418-425.
11. Majumder, S.; Neogi, S. Antimicrobial activity of copper oxide nanoparticles coated on cotton fabric and synthesized by one-pot method. *Adv. Sci. Eng. Med*. **2016**, 8, 102-111.
12. Nibret, A.; Yadav, O.P.; Diaz, I.; Taddesse, A.M. Cr-N co-doped ZnO nanoparticles: Synthesis, characterization and photocatalytic activity for degradation of thymol blue. *Bull. Chem. Soc. Ethiop.* **2015**, 29, 247-258.
13. Ehi-Eromosele, C.O.; Olugbuyiro, J.A.O.; Taiwo, O.S.; Bamgboye, O.A.; Ango, C.E. Synthesis and evaluation of the antimicrobial potentials of cobalt doped- and magnesium ferrite spinel nanoparticles. *Bull. Chem. Soc. Ethiop.* **2018**, 32, 451-458.
14. Lisiecki, I.; Pileni, M.P. Syntheses of copper nanoparticles in microemulsion and in reverse micelles. *J. Am. Chem. Soc*. **1993**, 115, 3887-3896.
15. Hajipour, M.J.; Fromm, K.M.; Ashkarran, A.A.; de Aberasturi, D.J.; de Larramendi, I.R.; Rajo, T.; Serpooshan, V.; Parak, W.J.; Mohmoudi, M. Antibacterial properties of nanoparticles. *Trends Biotechnol*. **2012**, 30, 499-511
16. Buckley, J.J.; Gai, P.L.; Lee, A.F.; Olivi, L.; Wilson, K. Silver carbonate nanoparticles stabilised over alumina nanoneedles exhibiting potent antibacterial properties. *Chem. Commun.* **2008**, 18, 4013-4015.
17. Marambio-Jones, C.; Hoek, E.M. A review of the antibacterial effects of silver nanomaterials and potential implications for human health and the environment. *J. Nanopart. Res.* **2010**, 12, 1531-1551.
18. Tran, N.; Mir, A.; Mallik, D.; Sinha, A.; Nayar, S.; Webster, T.J. Bactericidal effect of iron oxide nanoparticles on *Staphylococcus aureus*. *Int. J. Nanomed.* **2010**, 5, 277-283.
19. Lee, C.; Kim, J.Y.; Lee, W.I.; Nelson, K.L. Yoon, J.; Sedlak, D.L. Bactericidal effect of zero-valent iron nanoparticles on *Escherichia coli*. *Environ. Sci. Technol*. **2008**, 42, 4927-4933.
20. Lara, H.H.; Garza-Treviño, E.N.; Ixtepan-Turrent, L.; Singh, D.K. Silver nanoparticles are broad-spectrum bactericidal and virucidal compounds. *J. Nanobiotechnol*. **2011**, 9, 30. DOI: 10.1186/1477-3155-9-30.
21. Zhao, Y.; Tian, Y.; Cui, Y.; Liu, W.; Ma, W.; Jiang, X. Small molecule-capped gold nanoparticles as potent antibacterial agents that target gramnegative bacteria. *J. Am. Chem. Soc*. **2010**, 132, 12349-12356.
22. Jin, T.; He, Y. Antibacterial activities of magnesium oxide (MgO) nanoparticles against food borne pathogens. *J. Nanopart. Res*. **2011**, 13, 6877-6885.
23. Lellouche, J.; Friedman, A.; Lellouche, J.P.; Gedanken, A.; Banin, E. Improved antibacterial and antibiofilm activity of magnesium fluoride nanoparticles obtained by water-based ultrasound chemistry. *Nanomed-Nanotechnol*. **2012**, 8, 702-711.
24. Besinis, A.; De Peralta, T.; Handy, R.D. The antibacterial effects of silver, titanium dioxide and silica dioxide nanoparticles compared to the dental disinfectant chlorhexidine on *Streptococcus mutans* using a suite of bioassays. *Nanotoxicol*. **2014**, 8, 1-6.

25. Espitia, P.J.P.; Soares, N.F.F.; dos Reis Coimbra, J.S.; de Andrade NJ, Cruz, R.S.; Medeiros, E.A.A. Zinc oxide nanoparticles: Synthesis, antimicrobial activity and food packaging applications. *Food Bioprocess Technol.* **2012**, 5, 1447-1464.
26. Karthik, A.D.; Geetha, K. Synthesis of copper precursor, copper and its oxide nanoparticles by green chemical reduction method and its antimicrobial activity. *J. Appl. Pharm*. **2013**, 3, 016-021.
27. Premkumar, T.; Geckeler, K.E. A green approach to fabricate CuO nanoparticles. *J. Phys. Chem. Solids* **2006**, 67, 1451-1456.
28. Nakamoto, K. *Infrared Raman Spectra of Inorganic and Coordination Compounds*, 3rd ed., John Wiley and Sons: New York; **1992**.
29. Radhakrishnan, A.A.; Beena, B.B. Structural and optical absorption analysis of CuO nanoparticles. *Indian J. Adv. Chem. Sci.* **2014**, 2, 158-161.
30. Singh, I.; Bedi, R.K. Surfactant-assisted synthesis, characterizations, and room temperature ammonia sensing mechanism of nanocrystalline CuO. *Solid State Sci.* **2011**, 13, 2011-2018.
31. Srivastava, M.; Ojha, A.K.; Chaubey, S.; Sharma, P.K.; Pandey, A.C. *J. Alloy Compd.* **2010**, 494, 275-484.
32. Alt, V.; Bechert, T.; Steinrcke, P.; Wagener, M.; Seidel, P.; Dingeldein, E.; Domann, U.; Schnettler, R. An in vitro assessment of the antibacterial properties and cytotoxicity of nanoparticulate silver bone cement. *Biomater*. **2004**, 25, 4383-4391.
33. Furno, F.; Morley, K.S.; Wong, B.; Sharp, B.L.; Arnold, P.L.; Howdle, S.M.; Bayston, R.; Brown, P.D.; Winship, P.D.; Reid, H. Silver nanoparticles and polymeric medical devices: A newapproach to prevention of infection. *J. Antimicrob. Chemother*. **2004**, 54, 1019-1024.
34. Jeong, S.H.; Yeo, S.Y.; Yi, S.C. The effect of filler particle size on the antibacterial properties of compounded polymer/silver fibers. *J. Mater. Sci*. **2005**, 40, 5407-5411.
35. Chou, W.L.; Yu, D.G.; Yang, M.C. The preparation and characterization of silver-loading cellulose acetate hollow fiber membrane for water treatment. *Polym. Adv. Technol*. **2005**, 16, 600-607.
36. Sambhy, V.; MacBride, M.M.; Peterson, B.R.; Sen, A. Silver bromidenanoparticle/polymer composites: Dual action tunable antimicrobial materials, *J. Am. Chem. Soc*. **2006**, 128, 9798-9808.
37. Stoimenov, P.K.; Klinger, R.L.; Marchin, G.L.; Klabunde, K. Metal oxide nanoparticles as bactericidal agents. *Lang.* **2002**, 18, 6679-6686.
38. Hsiao, M.T.; Chen, S.F.; Shieh, D.B.; Yeh, C.S. One-pot synthesis of hollow Au3Cu1 spherical-like and biomineral botallackite Cu-2(OH)(3)Cl flowerlike architectures exhibiting antimicrobial activity. *J. Phys. Chem. B* **2006**, 110, 205-210.
39. Theivasanthi, T.; Alagar, M. Studies of copper nanoparticles effects on micro-organisms. *Annals Biol. Res*. **2011**, 2, 368-373.
40. Morones, J.R.; Elechiguerra, J.L.; Camacho, A.; Holt, K.; Kouri, J.B.; Ramírez, J.T.; Yacaman, M.J. The bactericidal effect of silver nanoparticles. *Nanotechnol.* **2005**, 16, 2346-2353.
41. Lee, C.; Kim, Y.; Lee, W.I.; Nelson, K.L.; Yoon, J.; Sedlak, D.L. Bactericidal effect of zero-valence iron nanoparticles on *Escherichia coli*. *Environ. Sci. Technol*. **2008**, 42, 4927-4933.
42. Zvekic, D.; Srdic, V.V.; Karaman, M.A.; Matavulj, M.N. Antimicrobial properties of ZnO nanoparticles incorporated in polyurethane varnish. *Proc. Appl. Cer*. **2011**, 5, 41-45.
43. Rajendran, R.; Bala Kumar, C.; Ahammed, H.A.M.; Jayakumar, S.; Vaideki, K.; Rajesh, E.M. Use of zinc oxide nanoparticles for production of antimicrobial textiles. *Int. J. Eng. Sci. Technol*. **2010**, 2, 202-208.
44. Gondal, M.A.; Dastageer, M.A.; Khalil, A.; Hayat, K.; Yamani, Z.H. Nanostructured ZnO synthesis and its application for effective disinfection *Escherichia coli* micro organism in water. *J. Nanopart. Res*. **2011**, 133, 423-430.

45. Wangsaprom, K.; Maensiri, S. Synthesis structural characterization of nickel oxide nanoparticles synthesized by polymerized complexed (PC) method, *Proceed in 3rd Int. Nanoelec. Conf*. **2010**, 1044-1045.
46. Kavitha, T.; Yuvaraj, H. A facile approach to the synthesis of high-quality NiO nanorods: Electrochemical and antibacterial properties. *J. Mater. Chem*. **2011**, 21, 15686-15691.
47. Perez, C.; Paul, M.; Bazerque, P. Antibiotic assay by agar well diffusion method, *Acta Biol. Med. Exp.* **1990**, 15, 113-115.